

# DS-CDMA MAI-CANCELLATION USING HYSTERETIC HOPFIELD NEURAL NETWORKS

EBRAHIM ALI SOUJERI

Department of E. E. Engineering, European University of Lefke  
Gemikonagi, North Cyprus

(Visiting Consultant of E. E. Eng., Sultan Qaboos University  
Muscat, Sultanate of Oman)

*esoujeri@ieee.org*

**Abstract** — Multi-user interference cancellation (MAI) using hysteretic Hopfield neural network (HHNN) receiver for direct sequence code-division multiple access (DS-CDMA) in multipath fading (MPF) channels is investigated. We have shown that by applying the phenomenon of “hysteresis” to the HNN detector, we may enhance the performance of this detector in all near-far situations for different number of multipath rays. The introduction of Hysteresis concept into HNN has made the CDMA HNN detector (which we shall call the HHNN detector) to have even a closer performance compared to the CDMA optimum multiuser detector. As shown by simulation results, the BER performance achieved by the HHNN detector outperforms the classical HNN detector with a good margin and is promising.

## I. INTRODUCTION

Hopfield neural network (HNN) multiuser detector is a nonlinear receiver whose complexity is linearly proportional to the number of users. The first work on CDMA detection using Hopfield neural network appeared in 1996 by Kechriotis and Manolakos [1], followed by works of Miyajima et. al. [2]. These Hopfield-based detectors were proposed for an AWGN channel. In light of conclusions drawn by these works, the Hopfield detector is known since then to have low complexity while achieving a BER performance very close to the optimum multiuser detector [1, 2].

In 2002 Soujeri et al showed that Hopfield detection can be also applied to multipath situations, where the signals arrive to the detector after passing through a multipath fading channel. In fact, Soujeri et al showed that it was the correct choice of the cross-correlation matrix and the channel state information (CSI) that enabled the HNN to detect CDMA signals in multipath situations [3, 4].

The concept of hysteresis was introduced into Hopfield neural networks by Bharitkar and Mendel in 2000 and showed that the Hysteretic HNN is stable in the sense of Lyapunov [5].

In this paper, enlightened by the work of Bharitkar, we have applied the Hysteretic Hopfield neural network

to the detection problem of DS-CDMA signals in multipath fading channels. Fortunately and as expected, we have come up with satisfying and promising results concerning BER performance enhancement using the HHNN CDMA multiuser detector.

## II. SYSTEM DESCRIPTION

### A. Transmitter Model

We assume that there are  $K$  transmitters in the system and each transmitter employs a binary phase-shift keying direct sequence spread spectrum (BPSK DS/SS) signal. The original data stream of user  $k$  (transmitter  $k$ ) are transmitted in packets of size  $P$  and are denoted as

$$\mathbf{b}_k = [b_{k,1} \quad b_{k,2} \quad \cdots \quad b_{k,P-1} \quad b_{k,P}] \in \{\pm 1\}^{1 \times P} \quad (1)$$

The overall transmitted CDMA data  $\mathbf{b}$  is a block or packet of size  $K \times P$  with duration  $T_s = PT_b$ , the matrix form of which can be expressed as

$$\mathbf{b} = \begin{bmatrix} b_{1,1} & \cdots & b_{1,P} \\ \vdots & \ddots & \vdots \\ b_{K,1} & \cdots & b_{K,P} \end{bmatrix} \in \{\pm 1\}^{K \times P} \quad (2)$$

The spreading code of the  $k$ th user is time-limited to one bit duration  $[0, T_b]$  and is given as

$$c_k(t) = A_k a_k(t) \cos(\omega_c t + \theta_k), \quad 0 \leq t \leq T_b \quad (3)$$

where  $A_k$  is the  $k$ th user's amplitude,  $\omega_c$  is the common carrier frequency,  $\theta_k$  is the phase angle of the  $k$ th user. The spreading signal  $a_k(t)$  is defined as

$$a_k(t) = \sum_{i=1}^L a_i^k u_{T_c}(t - (i-1)T_c) \quad (4)$$

where  $u_{T_c}(t)$  is the unit rectangular pulse of duration  $T_c$  and  $a_i^k \in \{\pm 1\} \quad \forall i, k$  is the spreading sequence whose length denotes the CDMA processing gain  $L = T_b/T_c$ . The received energy per bit of the  $k$ th user's signature waveform is denoted by  $E_k = A_k^2 T_b / 2$ .

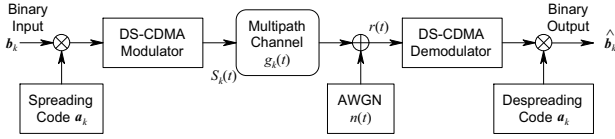


Figure 1. A general block diagram of the DS-CDMA system for the  $k$ th user.

A general block diagram of CDMA system for a single ( $k$ th) user is as shown in Fig. 1.

When the relative received power of the interfering signals become large, near-far problem arises and  $E_k$  changes for different users. The transmitted BPSK signal of user  $k$  is the product of information bits  $\mathbf{b}$  into spreading sequences  $\mathbf{c}$  and the overall transmitted signal for all users  $S(t)$  is the summation of individual signals sent by each user, which is written as

$$S(t) = \sum_{k=1}^K \sum_{p=1}^P b_{k,p} c_k(t - pT_b - \tau_k) \quad (5)$$

Here,  $b_{k,p} \in \{\pm 1\}$  is the  $p$ th transmitted bit of the  $k$ th user,  $P$  is the packet size and  $T_b$  is the bit interval duration and  $\tau_k \in [0, T_b)$  is the time delay of the  $k$ th user.

### B. Multipath Channel Model

Several multipath models have been used in the literature, varying from the very comprehensive one to the simple tapped delay line model [6]. In this paper, the MPF channel is modeled as consisting of a fixed number of resolvable Rayleigh faded paths. The low-pass impulse response of the channel for user  $k$  is given by [6]

$$g_k(t) = \sum_{\psi=1}^{\Psi} \beta_{k,\psi} e^{j\gamma_{k,\psi}} \delta(t - t_{k,\psi}) \quad (6)$$

where  $\Psi$  is an integer that represents the total number of resolvable paths,  $\delta$  is the famous delta-dirac function and  $t_{k,\psi}$  represents the channel delay of the  $\psi$ th path of user  $k$ . Here,  $\beta_{k,\psi}$  is a Rayleigh random variable and the angle  $\gamma_{k,\psi}$  is a uniform random variable in the interval  $[0, 2\pi)$ . Both  $\beta_{k,\psi}$  and  $\gamma_{k,\psi}$  are independent for different  $k$  and  $\psi$ . The product  $\beta_{k,\psi} e^{j\gamma_{k,\psi}}$  is a complex Gaussian random variable with zero mean and variance  $\sigma_{\psi}^2$ . Fading channel coefficients are assumed to have a variance normalized for convenience so that

$$E \left( \sum_{\psi=1}^{\Psi} |c_{k,\psi}|^2 \right) = 1, \quad \forall k \quad (7)$$

The channel described above is schematically shown in Fig. 2.

## III. MULTIUSER DETECTION OF CDMA SIGNALS

Assuming  $K$  active asynchronous CDMA users in the system, all using the same selection of  $P$  and  $L$ , the power received from each user at the base station is not necessarily the same even under no fading conditions because of near-far effect. The received signal in this MPF channel is given by

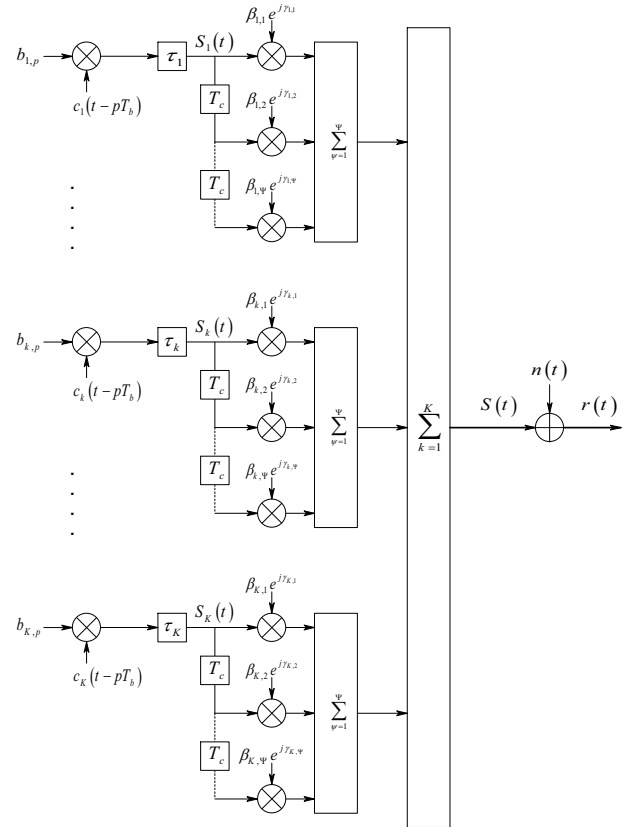


Figure 2. Block diagram of the  $p$ -path complex channel used in this work.

$$r(t) = n(t) + \sum_{k=1}^K g_k(t) \otimes S_k(t) \quad (8)$$

where ' $\otimes$ ' is the convolution operation and  $n(t)$  is AWGN with zero mean and two-sided power spectral density of  $N_0/2$ . The received signal in this channel can be written as

$$r(t) = n(t) + \sum_{k=1}^K \sum_{p=1}^P b_{k,p} \sum_{\psi=1}^{\Psi} \beta_{k,\psi} e^{+j\gamma_{k,\psi}} c_k(t - pT_b - \tau_k - t_{k,\psi}) \quad (9)$$

As seen,  $\Psi$  replicas of the transmitted signal arrive at the receiver through a total of  $\Psi$  paths, with a time delay of  $t_{k,\psi}$  seconds for the  $\psi$ th path. In our work in this paper, we have considered 1-ray, 2-ray, 3-ray and 5-ray channels, and we have assumed the arrival of 1 ray per path to the receiver. Therefore 3-ray channel also means 3-path channel.

### A. CDMA Correlator Detector Output

The correlator detector (CD) is the basic CDMA detector that consists of a bank of matched filters, used in de-spreading the transmitted CDMA signal to retrieve the transmitted data. The  $p$ th CD output of the  $k$ th user is expressed as

$$y_{k,p} = \int_{(p-1)T_b + \tau_k}^{pT_b + \tau_k} s_k^*(t - pT_b - \tau_k) r(t) dt \quad (10)$$

The channel considered in this case is a frequency non-selective slowly fading one such that the  $\psi$ th path

gain  $\beta_{k,\psi}$  and phase rotation  $\gamma_{k,\psi}$  are constant at least over one packet duration  $T_s = PT_b$ . Combining of multipath reflections is considered to be an integral part of the despreading operation. To achieve maximum ratio combining (MRC) of the multipath reflections, one could justify that for perfect matching,  $s_k^*(t)$  in (10) must be [3]:

$$s_k^*(t) = \sum_{\psi=1}^{\Psi} \beta_{k,\psi} e^{-j\gamma_{k,\psi}} c_k(t - t_{k,\psi}) \quad (11)$$

### B. Mechanism of Optimum Detection

The optimum multiuser detection considers the optimum multiuser demodulation of  $PK$  bits, which includes data from the 1st bit to the  $P$ th bit of all the  $K$  active users in the system, where  $P$  is the packet size. The reason to consider the optimum data demodulation is to derive a corresponding suboptimum receiver with lower complexity. Since the noise is white and Gaussian and all the transmitted data sequences are assumed to be equi-probable, the maximum-likelihood sequence detector selects the estimates of the data sequence expressed in vector form  $\hat{\mathbf{b}}_p = [\hat{b}_{1,p}, \dots, \hat{b}_{K,p}]^T$ ,

for  $1 \leq p \leq P$ , where  $[\cdot]^T$  stands for the transpose operation. The estimation is done by minimizing the Euclidean distance  $d_E$  between the received signal  $r(t)$  and the estimate of the transmitted signal  $\hat{S}(t)$ . The terms  $d_E$  and  $\hat{S}(t)$  can be respectively expressed as

$$d_E = \int_0^{T_s} |r(t) - \hat{S}(t)|^2 dt \quad (12)$$

$$\hat{S}_k(t) = \sqrt{E_k} \sum_{p=1}^P \hat{b}_{k,p} \sum_{l=1}^L a_{k,l} \quad (13)$$

Minimization of the Euclidean distance given in Eq. (12) is expressed as in Eq. (14) in terms of the likelihood function  $\Lambda$  that is given by Eq. (15) [6, 7].

$$\hat{\mathbf{b}}_{\text{OMD}} = \text{Arg} \left[ \text{Min}_{\mathbf{b} \in \{\pm 1\}^{PK}} (\text{Re}\{\Lambda\}) \right] \quad (14)$$

$$\Lambda = -\mathbf{y}^T \mathbf{b} + \frac{1}{2} \mathbf{b}^T \mathbf{H} \mathbf{b} \quad (15)$$

Where  $\mathbf{y} \in \mathbb{C}^{1 \times PK}$  in Eq. (15) is the MF output with its  $k$ th element as given in Eq. (10) and  $\mathbf{b} \in \{\pm 1\}^{PK \times 1}$  is a pool in which the optimum detector searches for  $\hat{\mathbf{b}}_{\text{OMD}} \in \{\pm 1\}^{PK \times 1}$ . The optimum detection algorithm finds an estimate  $\hat{\mathbf{b}}_{\text{OMD}}$  by substituting a stream  $\mathbf{b}$  into  $\Lambda$  such that the real part of  $\Lambda$  is minimized. The stream  $\mathbf{b}$  begins with  $\mathbf{b} = [-1 \ -1 \ \dots \ -1]^T \in \{-1\}^{PK \times 1}$  and ends up with  $\mathbf{b} = [1 \ 1 \ \dots \ 1]^T \in \{+1\}^{PK \times 1}$ ; for every  $\mathbf{b}$ , the algorithm stores the value of  $\text{Re}\{\Lambda\}$ , and after finishing with all streams, the algorithm checks which stream resulted in a minimum value for  $\text{Re}\{\Lambda\}$  and chooses that stream as  $\hat{\mathbf{b}}_{\text{OMD}}$ . The OMD detector has a complexity in the order of  $2^{PK}$ . This complexity is high

since the product of number of users into the packet size is very high, i.e.  $PK \gg 1$ . Inapplicability of the optimum detector for practical CDMA communications has led people in the field to search for alternative CDMA detectors [1, 6].

### C. Mechanism of HNN Detection

We consider  $K$  users who transmit  $P$  bits in parallel, so, the relevant number of inputs to hnn detector is  $PK$ . the bias vector  $\mathbf{I} = [I_1 \ I_2 \ \dots \ I_{PK}]^T$  and the interconnection matrix  $\mathbf{T}$  of HNN [3, 4] is taken from the communication system parameters. HNN output vector is denoted by  $\mathbf{V} = [V_1, \dots, V_{PK}]^T$ . A simple 5-neuron model of the HNN detector that has been deployed as a CDMA detector in this work is shown in Fig. 3. Hopfield has shown that if interconnection weights are symmetric ( $T_{qi} = T_{iq}$ ), the state of the network always converges to a stable state [8]. The stable states of the network are the minima of the energy function of HNN described by

$$E_{\text{HNN}} = -\sum_{i=1}^{PK} V_i I_i - \frac{1}{2} \sum_{i=1}^{PK} \sum_{j=1}^{PK} V_i T_{ij} V_j \quad (16)$$

Once the output of HNN at a certain iteration is determined, back propagation starts to update the states of HNN nodes for next iteration. Considering that the states of HNN change as their dynamics change, this change is best characterized by the equation of motion of the HNN neurons which is given by [1, 2]

$$\frac{dU_i(t)}{dt} = -\left( \frac{\partial E_{\text{HNN}}}{\partial V_i} + \frac{U_i(t)}{\tau} \right) \quad (17)$$

Considering the discrete-time approximation of  $d/dt(U_i(t))$  that is given by

$$\frac{dU_i(t)}{dt} = \frac{U_i(t + \Delta t) - U_i(t)}{\Delta t} \quad (18)$$

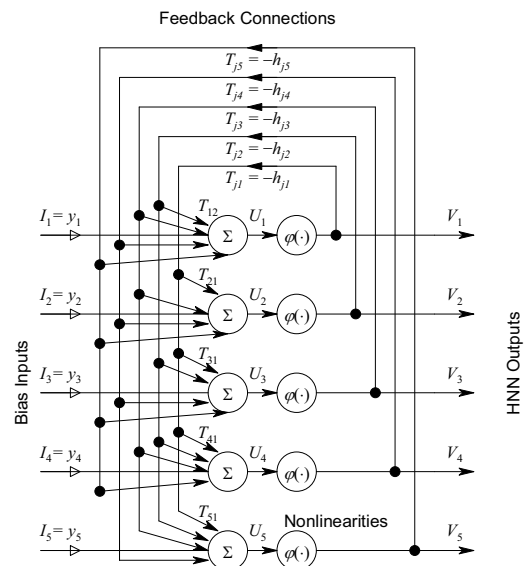


Figure 3. Interconnection diagram of 5-neuron HNN.

and letting  $\Delta t = 1$ , we can express the above change as

$$\Delta U_i(n) = U_i(n+1) - U_i(n) \quad (19)$$

which leads to

$$U_i(n+1) = \Delta U_i(n) + U_i(n) \quad (20)$$

where  $n$  represents the discrete time index.

Noting that  $\frac{\partial E_{\text{HNN}}}{\partial V_i} = -\sum_{j \neq i} T_{ij} V_j - I_i$ , the expression in

Eq. (19) may be rewritten as

$$\Delta U_i(n) = \sum_{j \neq i} T_{ij} V_j + I_i - \frac{1}{\tau} U_i(n) \quad (21)$$

where  $\tau = RC$  is the time-constant of HNN neurons used in VLSI design [1]. The expression given in Eq. (21) represents the change in HNN states at the  $n$ th iteration. We may now transform the minimization of the likelihood function given in Eq. (15) into the minimization of HNN energy function that is described in Eq. (16) by setting HNN biases  $\mathbf{I}$  as MF outputs  $\mathbf{y}$ , and interconnections  $\mathbf{T}$  as cross-correlations of spread sequences  $\mathbf{H}$  as below

$$\mathbf{I} = \mathbf{y} \quad (22)$$

$$\mathbf{T} = -\mathbf{H} \quad (23)$$

Once the transformations given in Eqs. (22–23) are done, HNN is operated for sufficient iterations, typically around 10 iterations or until convergence is established. The data estimate  $\hat{\mathbf{b}}_{\text{HNN}}$ , could be simply driven by hard-limiting the real part of HNN output  $\mathbf{V}$ , as follows

$$\hat{\mathbf{b}}_{\text{HNN}} = \text{sgn}\{\text{Re}(\mathbf{V})\} \quad (24)$$

Here, the output vector  $\mathbf{V} \in \mathbb{C}^{PK \times 1}$  is obtained after the network has reached a stable state by performing the necessary number of iterations required. The block diagram of the complete CDMA receiver that utilizes HNN detector based on Eqs. (22–24) is given in Fig. 4.

#### IV. THE HYSTERETIC HOPFIELD NEURAL NETWORK

In this section we examine the performance of the HNN multiuser detector for asynchronous DS-CDMA transmissions in a multipath channel.

##### The Hysteretic Hopfield Neural Network (HHNN)

Bharitkar and Mendel [5] proposed a Hopfield neural network model that is based on the phenomenon of hysteresis. We have used the idea in [5] to develop the HHNN CDMA detector.

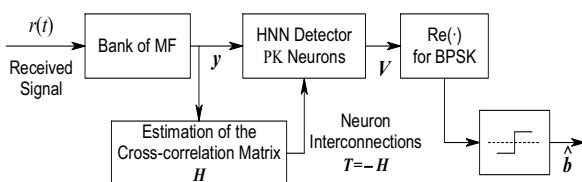


Figure 4. The HNN detection for multiuser CDMA.

#### The Hysteretic Neuron

The hysteretic neuron is similar to other neuron models in that it processes a linear weighted combination of inputs. It differs from other neuron models in that its nonlinear activation function is the hysteresis function [5] that is depicted in Fig. 5. Mathematically, the output of the hysteretic neuron  $V$  depends on the decision taken by the hysteretic neuron activation function, given by the neuron state and conditioned on the change in the neuron input or state  $U$ , as described below

$$V(U(t)|\dot{U}(t-\delta t)) = \varphi(U(t) - \lambda(\dot{U}(t-\delta t))) \quad (25)$$

Where  $\varphi(U) = \tanh(\gamma U)$  and

$$\gamma(\dot{U}(t-\delta t)) = \begin{cases} \gamma_{\alpha_h}, & \dot{U}(t-\delta t) \geq 0 \\ \gamma_{\beta_h}, & \dot{U}(t-\delta t) < 0 \end{cases} \quad (26)$$

$$\lambda(\dot{U}(t-\delta t)) = \begin{cases} -\alpha_h, & \dot{U}(t-\delta t) \geq 0 \\ +\beta_h, & \dot{U}(t-\delta t) < 0 \end{cases} \quad (27)$$

In the above,  $\beta_h > -\alpha_h$ , the group  $\{\gamma_{\alpha_h}, \gamma_{\beta_h}\} > \{0, 0\}$  and  $\dot{U}(t-\delta t)$  is by definition, the first derivative of  $U(t)$  with respect to time, given by

$$\dot{U}(t-\delta t) \triangleq \frac{dU(t-\delta t)}{dt} = \lim_{\delta t \rightarrow 0} \frac{U(t) - U(t-\delta t)}{\delta t} \quad (28)$$

Conditioned upon the change  $\dot{U}(t-\delta t)$  in Eqs. (26–27) above, the function  $\gamma$  determines the crosspoint of the hysteresis with respect to  $\dot{U}(t-\delta t)$  and the function  $\lambda$  determines the gain to be used by the activation function with respect to  $\dot{U}(t-\delta t)$ . The function  $\gamma$  chooses the gain  $\gamma_{\alpha_h}$  when the change  $\dot{U}(t-\delta t)$  is positive and chooses the gain  $\gamma_{\beta_h}$  when the change is  $\dot{U}(t-\delta t)$  negative. The function  $\lambda$  chooses the hysteresis located on the crosspoint  $-\alpha_h$  for a positive change  $\dot{U}(t-\delta t)$  and chooses the crosspoint  $\beta_h$  for a negative change  $\dot{U}(t-\delta t)$ .

In a non-hysteretic HNN structure, the degree of nonlinearity of the sigmoid function represented by  $\varphi(\cdot)$  is dependent on the value of  $\alpha$ . Note that if  $\alpha \rightarrow \infty$ , then  $\varphi(\cdot) \rightarrow \text{sign}(\cdot)$ . In the special case when  $\beta_h = \alpha_h$  and  $\gamma_{\alpha_h} = \gamma_{\beta_h}$ , the activation function becomes the conventional sigmoid. Observe that the neuron's output not only depends on its input  $U$ , but also on derivative information  $\dot{U}$ . It is the derivative information that provides the neuron with memory and distinguishes it from other neuron models. From Eqs. (25–28), if  $U$  is positive at a discrete time and increases in value at the next discrete time, the activation function remains along the segment A – B.

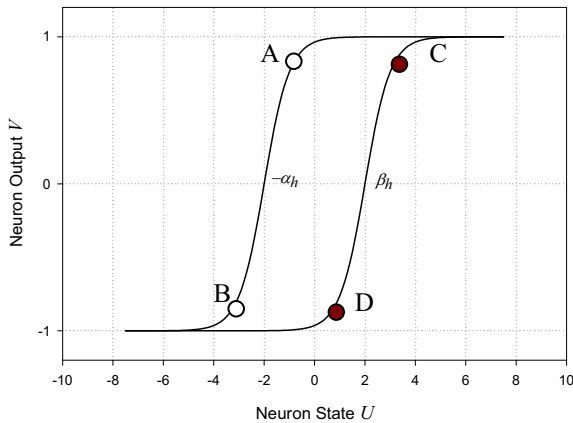


Figure 5. The hysteretic activation function in HHNN consists of two hyperbolic tangent functions centered at  $-\alpha_h$  and  $\beta_h$ .

On the other hand, if  $U$  is positive at a discrete time and decreases at the next discrete time, then the activation function jumps from hysteretic segment A – B to hysteretic segment C – D. The hysteretic activation function along with the two segments A – B and C – D are shown in Fig. 5. Note that the hysteretic neuron’s activation function has four parameters associated with it, namely,  $\alpha_h, \beta_h, \gamma_{\alpha_h}$  and  $\gamma_{\beta_h}$ . If the HNN is optimised with respect to these parameters, then, the probability of convergence into the global minimum is increased. Usually, one does not tune an ordinary neuron’s activation function, because for the most part, there are no parameters to tune (or there is at most one parameter, the slope of the sigmoid). The hysteretic neuron is different in this sense, and we can think about tuning all of its parameters in order to maximize its performance. So, it seems that the hysteretic neuron is much more flexible than the usual neuron. As a matter of fact, the hysteretic neuron can be applied to many types of neural networks such as multilayer neural network and recurrent neural network. In this paper, we apply it to the Hopfield neural network. Moreover, more details on a RC circuit-based noiseless dynamical model of the hysteretic neuron are found in Bharitkar [5].

Unlike the usual HNN, the HHNN includes memory. Memory is necessarily needed to determine the change  $\dot{U}_j(t - \delta t)$ . It is the attractive features of the HHNN which encourages us to study the performance of this type of neural network as a CDMA detector. Note that in the ordinary (non-hysteretic) HNN,  $\alpha_h = \beta_h = 0$ .

### V. SIMULATION RESULTS

Comprehensive and extensive computer simulation have been carried out to demonstrate the performance of *hysteretic* HNN CDMA detector. Simulation is mainly divided into two parts. The first part demonstrates the performance of CDMA with respect to near-far-ratio; for which the BER results of the desired user (the 1<sup>st</sup> user) are plotted with respect to the near far ratio  $E_i/E_1$  in decibels (dB). In this case, the desired user is the first user with energy  $E_1$ , and the interference is caused by the other users who are the 2<sup>nd</sup> to the  $K^{\text{th}}$  users with

energies  $E_2=E_3=\dots=E_K$ . The ratio  $E_i/E_1$  stands for the amount of relative interference caused by undesirable users. A positive (negative) dB value of  $E_i/E_1$  means that interference is stronger (weaker) than desired user’s signal. The second part demonstrates the performance of CDMA with respect to signal-to-noise ratio  $E_1/N_0$  in decibels (dB); for which the average BER results for all users are plotted with respect to the signal to noise ratio (SNR)  $E_1/N_0$  in dB. In the second case, all users are assumed to have equal energies, i.e.  $E_1=E_2=E_3=\dots=E_K$ , and the average BER is plotted.

In all simulation carried out in this work, performance of the matched-filter based correlator detector (CD) and the multistage detector (MSD) are also shown for its relevance to the HNN detector. In fact, performance of the CD detector is customarily shown in multiuser detection problems for the purpose of comparison and reference. This is because all research about suboptimum multiuser detection has emerged after the CD had failed to combat in near-far situations.

We have used the following values throughout our simulation,  $K=10$  users,  $L=15$  chips/bit and  $P=4$  bits/packet. In the first part of the simulation, where near-far-ratio is our concern, SNR =7.5 dB and each simulation is averaged over 2,000,000 bits. In the second part of the simulation, where SNR is our concern,  $E_i/E_1=0$  dB and number of simulated bits vary according

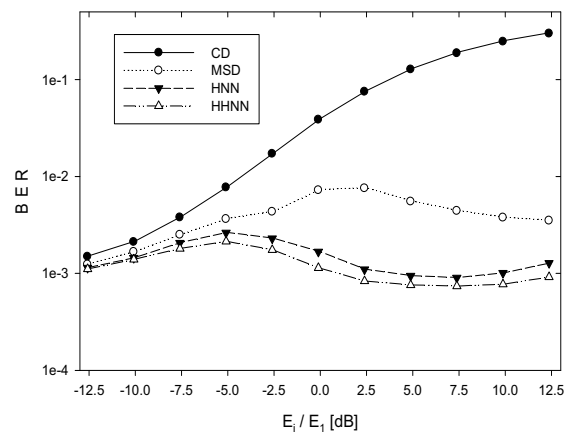


Fig. 6. Near-far Performance for 5-path fading channel.

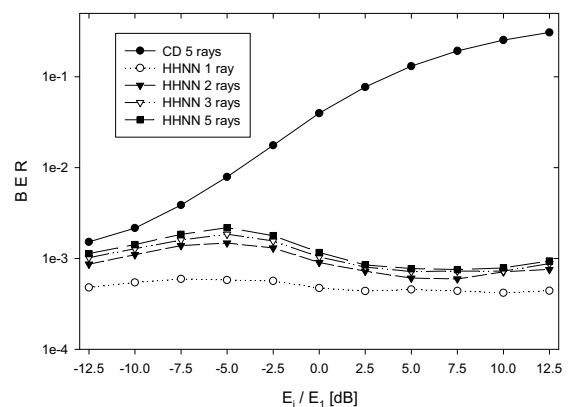


Fig. 7. Performance for different number of multipath rays.

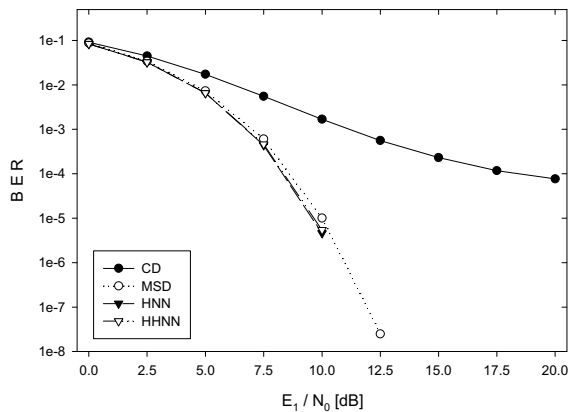


Fig. 8. BER performance vs. SNR in a single-path fading channel.

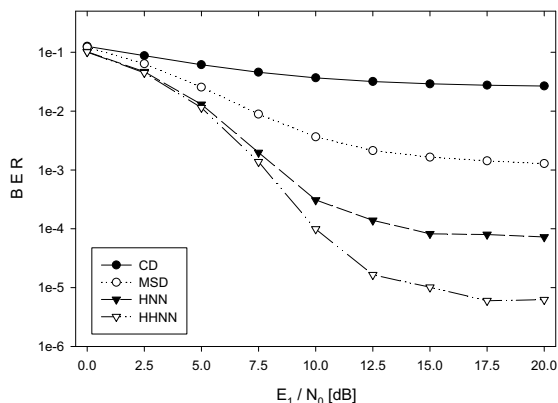


Fig. 9. BER performance vs. SNR in a 5-ray multipath fading channel.

to minimum BER requirements. Fig. 6 compares the performance of HHNN to HNN, MSD and CD for a 5-path system vs. near-far ratio and Fig. 7 shows the effect of multipath on performance for the HHNN detector. Fig. 8 and Fig. 9 compare the performance of HHNN to HNN, MSD and CD for a single-path and 5-path channel vs. SNR (See how HHNN outperforms at multipath situations). Finally Fig. 10 shows the effect of multipath on the performance for the HHNN detector.

## VI. CONCLUSIONS

In this paper, we have applied the Hysteretic Hopfield neural network to the detection problem of DS-CDMA signals in MPF channels and have come up with satisfying results over BER performance enhancement. However, the performance improvement does not occur for any arbitrary location of  $\alpha_h$  and  $\beta_h$  on the sigmoid function. Here, we have used [9]

$$\alpha_h = \beta_h = 4 \text{diag}(\mathbf{H}) / L \quad (29)$$

to minimize the BER and enhance performance. Moreover, we can achieve BER performance improvement almost in all near-far situations and is independent of the number of multipath rays resolved at the receiver. Like the other parameters of the HNN, the Hysteretic parameter is also dependent on CDMA parameters.

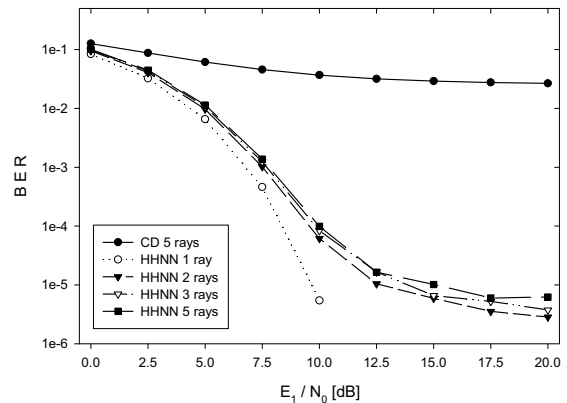


Fig. 10. Performance for different number of multipath rays versus SNR.

Therefore, the location of  $\alpha_h$  and  $\beta_h$  is dynamically updated when a change occurs in the CDMA system. The introduction of the concept of Hysteresis into HNN, has made the CDMA HNN detector (HHNN detector) even closer to the CDMA optimum multiuser detector. The BER performance achieved by the HHNN detector is promising.

## REFERENCES

- [1] G. I. Kechriotis and E. S. Manolagos, Hopfield Neural Network Implementation of the Optimal CDMA Multiuser Detector, *IEEE Trans. Neural Networks*, vol. 7, January 1996, 131-141.
- [2] T. Miyajima and T. Hasegawa, Multiuser Detection Using a Hopfield Network for Asynchronous Code-Division Multiple-Access Systems, *IEICE Trans. Fundamentals*, vol. E79-A, December 1996, 1963-1971.
- [3] E. Soujeri and Huseyin Bilgekul, Hopfield Multiuser Detection of Asynchronous MC-CDMA Signals in Multipath Fading Channels, *IEEE Communications Letters*, Vol. 6, No. 4, April 2002, 147-149.
- [4] E. Soujeri and Huseyin Bilgekul, Multiuser Detection of Synchronous MC-CDMA in Multipath Fading Channels Using Hopfield Neural Networks, *Kluwer Academic Publishers Neural Processing Letters*, Vol. 18, No. 8, August 2003, 49-63.
- [5] S. Bharitkar and J. M. Mendel, The Hysteretic Hopfield Neural Network, *IEEE Transactions on Neural Networks*, Vol. 11, No. 4, July 2000, 879-888.
- [6] A. Duel-Hallen, J. Holtzman and Z. Zvonar, Multiuser Detection for CDMA Systems, *IEEE Personal Communications*, April 1995.
- [7] A. Duel-Hallen, J. Holtzman and Z. Zvonar, Multiuser Detection for CDMA Systems, *IEEE Personal Communications Magazine*, Vol. 3, No. 4, May 1995, 46-58.
- [8] Hopfield, J.J., Neurons With Graded Response Have Collective Computational Properties Like Those of Two State Neurons, *Proceedings of National Academic Sciences, USA*, Vol. 81, 1984, 3088-3092.
- [9] E. Soujeri, *Ph.D Thesis*, Eastern Mediterranean University, Cyprus, September 2003.